Research article

Experimental Analysis of the Cooling Performance of A Fresh Air Handling Unit

Yousef Al Horr and Bourhan Tashtoush*

Gulf Organisation for Research and Development, Qatar Science and Technology Park, P.O. Box 210162, Doha, Qatar

* Correspondence: Email: b.taschtouch@gord.qa; Tel: +97455668259; Fax: +97444049002.

Abstract: An experimental investigation of the performance of a fresh air handling unit integrating indirect evaporative and vapor compression cooling is conducted. Temperature and relative humidity measurements at main points within the cooling unit were logged using a wireless data acquisition system. Experimental data downloaded from the acquisition system is used for linear regression analysis, and to calculate the wet-bulb thermal effectiveness, cooling capacity and coefficient of performance of the unit. The air conditioning unit is a patented system designed and assembled at the Gulf Organisation for Research and Development (GORD) in Qatar. The peak wet-bulb thermal effectiveness of the system was found to be 1.3, and the COP was 3.4. The results showed that the unit could save as nearly 60% of the sensible cooling load required by a conventional vapor compression cooling unit. In addition, the unit could reduce power consumption by 36% when utilizing the indirect evaporative cooling cycle. Depending on ambient conditions, the investigated unit generated enough condensate to meet the water requirements of the indirect evaporative cooling cycle, which made the air conditioning system sustainable.

Keywords: indirect evaporative cooling; temperature effectiveness; energy saving; Wet-bulb thermal effectiveness; condensate generation

Nomenclature: COP: Coefficient of Performance; DEC: Direct evaporative cooling; DX: Direct expansion; DX + WS: Direct expansion and water shower; E/A: Extract air; EAF: Extract air fan; FAHU: Fresh air handling unit; EC: Evaporative cooling; IDEC: Indirect, direct evaporative cooling; IEC: Indirect evaporative cooling; RH: Relative humidity; MVC: Mechanical vapour compression; P_{DX}: Power consumption of DX cooling cycle; P_{fans}: Power consumption of fans; P_{pumps}: Power

consumption of pumps; Q: Total cooling load (kW); S/A: Supply air; SAF: Supply air fan; T/H: Temperature and humidity sensor; T/S: Temperature sensor; $\in wbT$: Wet-bulb thermal effectiveness; ΔT: Temperature difference; ΔT_{HX}: Temperature difference across the heat exchanger; ΔT_{DX}: Temperature difference DX cooling coil

1. Introduction

Energy consumption due to air-conditioning applications in residential buildings in hot and humid or dry climates combined with the need to provide outdoor cooling in places such as walkways, stadiums, and external seating spaces for some restaurants drives, is significant. It is reported that the electrical load for cooling residential buildings alone approaches 70% of the total energy consumption. This vast energy consumption means that air conditioning of buildings contributes vast amounts of carbon dioxide and GHG emissions, which have a substantial adverse impact on the environment. The current use of energy in such proportions is unsustainable, therefore, to control and limit this exploding use of energy, there is a coordinated, but challenging, global effort to drive towards green buildings.

Globally, buildings account for more than 60% of the total consumption of energy, where residential facilities account for 40%; however, it varies from country to country as reported by several researchers [1–3]. The residential sector alone in the Middle East takes up 70% of the buildings energy consumption [4]. From a research perspective, significant effort is expended in investigating and developing new solutions for cooling and air conditioning of buildings. The research effort included the investigation of the utilization of renewable solar and other forms of waste energy in air conditioning cycles and using new refrigerants to enhance the system performance and have a compact refrigeration system [5–8]. One of the most significant recent developments in this area is the evolution of indirect evaporative cooling (IEC) systems. These are energy-efficient and eco-friendly substitutes for traditional vapor-compression air conditioning systems [9,10]. IEC systems come in a variety of configurations described mainly by the processes of heat and mass flow in the plate heat exchanger, i.e. parallel flow [11,12], counter-flow, crossflow, and other heat surface geometry that would enhance the heat transfer rate and improve the system performance [13–15]. The study of IEC systems attracts interest from many angles, including cooling capacity, wet-bulb thermal effectiveness, coefficient of performance, energy saving, water and power consumption, carbon dioxide, and others. While some researchers have focussed on experimental studies, others have pursued the development of mathematical models in the study of IEC systems. Evaporative cooling highly depends on climatic conditions and, several studies in the literature cover the application of IEC in hot/dry and hot/humid climates.

In recent years, there have been notable advancements in other types of IEC systems, such as the revolutionary Maisotsenko Cycle or M-Cycle and different regenerative configurations [16,17].

The IEC performance in hot climates was investigated and reported that the application of IEC as a pre-cooling module in air conditioning systems in humid and hot climates is still at a developing stage [18,19]. Simulation of a cooling cycle based on indirect/direct evaporative cooling (IDEC) was provided to estimate the performance characteristics of the system [20,21]. The simulation provided a way to estimate the performance characteristics of the system. Also, they showed that the COP of the combined system was 120% better than the performance of separate configurations. Substantial temperature reductions (up to 25 °C) of the air flowing across the heat exchanger could be achieved

with specific configurations of evaporative cooling systems, irrespective of the wet-bulb temperature of ambient air, and a simplified linear regression model of an IEC system using experimental data [22,23]. The arrangement of components in an IEC unit affects the performance of the unit and the behavior of the heat exchanger for simultaneous cooling and dehumidification. The results of a comparison with a phenomenological model showed only minor deviations (less than 5%) from which they concluded that their model could be appropriate to be executed in simulation software tools for evaporative cooling [24,25]. The effect of water spray configuration on the performance of an indirect evaporative cooling ventilation system was investigated, and the results indicated that the combined mode of operation performed better than the other two modes [26].

Furthermore, various types of materials could be used as a medium in IEC systems were studied to find their ability to hold shape, compatibility with a waterproofing coating, durability, compatibility with, risk of contamination as well as cost, are more significant than the thermal properties [27,28]. An analytical assessment of the energy-saving ability of and IEC compared to a traditional packaged air-conditioning unit was presented, and the results showed that the power requirement of the conventional package unit is 4.5 times more than is required for the IEC, to produce the same amount of cooling capacity [29]. Experimental and theoretical investigations were conducted to evaluate the system performance based on an IEC to pre-cool air for a conventional packaged air conditioning unit. It was found that the combined system saved more than 60% of the cooling load relative to the traditional air-conditioning unit [30,31]. The energy consumption of an IEC unit for fresh air-conditioning applications was analysed, and it was reported that the electrical load on the system was reduced by 80% compared to the demand for a traditional refrigerant-based cooling system [32].

Water consumption is the main downside of evaporative cooling techniques in engineering applications and air conditioning units. Researchers such as [33,34] have investigated water consumption aspects of the use of indirect evaporative cooling. Some reports suggested that the cooling capacity of the IEC heat exchanger, sprayed with only 0.004 $kg.s^{-1}$ of water, was twice as much as that obtained when the heat exchanger operates in dry mode.

In light of the above mentioned state-of-the-art literature review, there is still a lack of knowledge in water usage in different modes of operation (direct expansion (DX), water shower, or the combination of DX and water shower) in the evaporative cooling system that is used in different climatic conditions. Therefore, the present study aims at investigating and identifying the best operation mode with the least amount of water consumption at the prevailed ambient conditions. Furthermore, it is of interest to address the water consumption in the evaporating cooling systems for hot and arid ambient conditions experienced in GCC countries, and particularly in Qatar. The availability of such information will help in the selection of the best operating sequence and control of the evaporating cooling system to save water.

The present study investigates the cooling performance and energy savings of a new air handling technology, which was patented by Gulf Organisation for research and Development (GORD) in Qatar when operating in a variety of ambient conditions. The new technology integrates direct expansion (DX) cooling and IEC cycles. This study aims to pave the way for the development of a complete sequence of operation of the new technology. The most efficient combination of operating parameters will be investigated to find the minimum energy consumption and maximum condensate generation. The amount of condensed water is evaluated to off-set potable water requirements when the machine works in diverse ambient conditions. Different combinations of operating conditions,

including water shower and evaporative cooling, will be studied to find the best performance of the machine. The performance of the unit will be evaluated based on experimental data collected during the testing of the machine in the summer season in Qatar, and the energy utilization index (EUI) and energy cost index (ECI) of the new technology will be estimated.
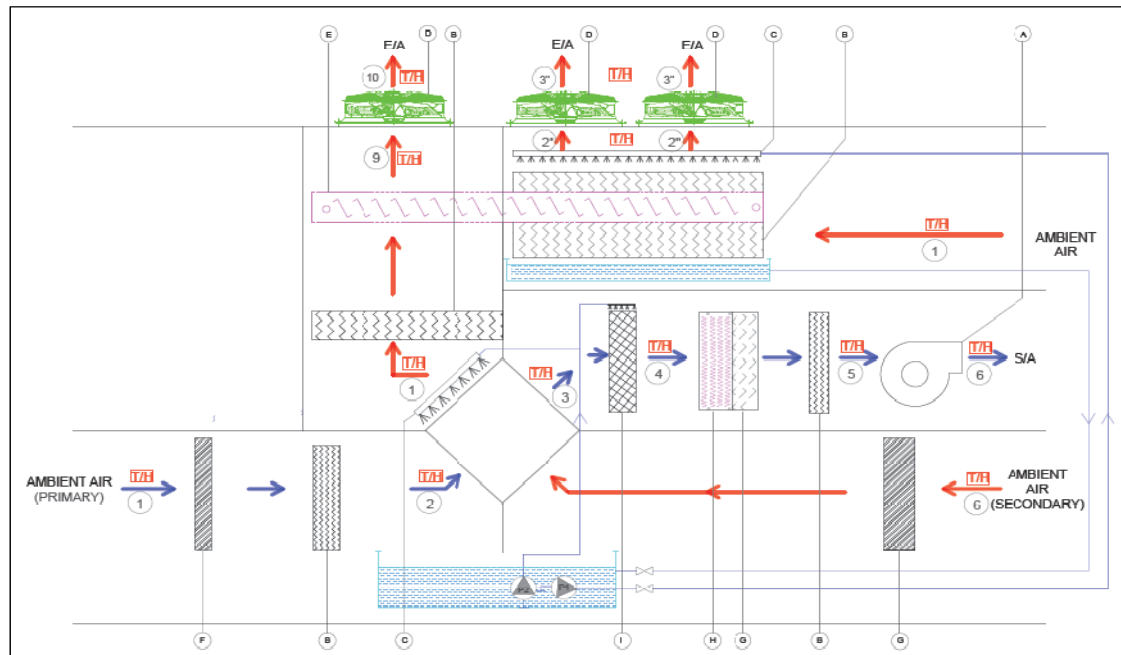
2. Experimental test setup

The air handling unit was designed, developed, and assembled by researchers at GORD. The air unit is a new type of air handling unit that uses next-generation cooling technologies. It incorporates IEC and IDEC cycles, integrated with a vapour compression cooling with DX. In this work, ways to enhance the energy efficiency and water-saving potential of the cooling unit are investigated.

Figure 1 shows a schematic diagram of the fresh air handling unit with a legend of all points. Primary airstream at ambient condition (state 1) drawn by the supply air fan enters the heat exchanger (state 2) and flows through the dry channels in the crossflow heat exchanger in which it is cooled by conduction as a result of the interaction with the cold surfaces of the heat exchanger (state 3). The primary airstream (state 3) flows across the direct evaporative cooling water shower, which is utilized to increase the humidity in cases when the ambient air is too dry (state 4). The temperature of the primary air is further reduced as it flows across the DX evaporator coil (state 5). The primary airstream flows across the supply air fan, gaining heat and reaches the desired supply air condition (state 6) pre-determined as the set-point.

The secondary airstream is drawn into the exhaust section of the air handling cooling unit at ambient condition (state 7). The secondary airstream undergoes evaporative cooling within the wet channels of the heat exchanger, thereby reducing the temperature of the primary airstream by indirect evaporative cooling. The secondary airstream leaving the heat exchanger (state 8) cools down the condenser of the DX cooling system, which warms the airstream (state 9) before it is discharged to the atmosphere (state 9).

The air handling cooling unit is also fitted with a separate cycle that can cool the vapor compression system condenser evaporatively by using a water shower. A simplified self-explanatory schedule of components included in the unit is given in Table 1.

Figure 1. Schematic diagram of the experimental set-up with the sensors.

Table 1. Schedule of main parameters of the experimental test rig.

Supply air fan	Centrifugal type. Airflow 13,000 CFM
DX Evaporator (R-410A)	8 rows, 13 fins per inch. Evaporator motor 2 at 5.7 kW
DX Condenser	Axial flow with 900 RPM
Extract air fan	13,000 CFM
Heat exchanger	Aluminum Crossflow type, plate thickness 0.15 mm, plate conductivity 0.22 kW.m^{-1} K^{-1}
Water shower pump	Submersible pump: flowrate 5.5 kg.s^{-} at 17.4 m
Condenser water pump	Submersible pump: flowrate 0.67 kg.s^{-1} at 38 m

3. Experimental methodology

The experiments are conducted at a fixed volumetric flow rate of 13000 CFM for the supply and secondary air flows. The water shower and condenser pump flow rates are 5.5 and 0.67 kg.s^{-1}, respectively. The setpoint temperature and relative humidity of the supply air are set at 16 °C an 50%, respectively. Values of temperature and relative humidity at pre-determined vital points within the

air handling cooling unit are measured using Aranet wireless sensors and logged onto a server. The temperature sensors have a range of −40 °C to 60 °C and accuracy of 0.4 °C, while the relative humidity sensor has a range of 0 to 100% with an accuracy of ±0.5%. Power consumption is measured with an energy meter. Data from experimental measurements are utilized for calculating various parameters that are used for comparing the performance of different cooling cycles. The thermal performance of evaporative cooling units is often linked to heat and mass processes. In the present study, the cooling performance of the unit is evaluated using parameters defined by the following expressions:

(i) wet-bulb thermal effectiveness, ϵ_{wbT}:

$$\epsilon_{wbT} = \frac{T_{o1} - T_{o2}}{T_{o1} - T_{wb1}} \tag{1}$$

(ii) The total cooling load is:

$$Q = m * (h_{01} - h_{02}) \tag{2}$$

where Q is the cooling load, h_{01} and h_{02} are the supply air enthalpies at states 1 and 2, respectively.

(iii) The Coefficient of Performance, COP is:

$$\text{COP} = \frac{Q}{P_{fans} + P_{pumps} + P_{DX}} \tag{3}$$

where P_{fans}, P_{pumps}, and P_{DX} are the power consumed by fans, pumps, and the compressor of the DX.

In the case of DX only operation, the quantity P_{pumps} is equal to zero.

Linear regression analysis is used to model and represent variations of various aspects of the cooling performance of the unit, i.e., temperature reduction across the heat exchanger, temperature reduction across the DX cooling coil, wet-bulb thermal effectiveness, coefficient of performance and cooling. It is defined as one of the well known statistical methods implemented for finding a relationship between a dependent and one or more independent variables. The dependent variable, in this analysis, is the temperature difference, $T_{HX,}$ while the ambient temperature and relative humidity are the independent variables. The linear regression analysis adopted here aims at finding the relationship's strength between the dependent and independent variables. This can be used in modeling the future relationship between them. The linear regression model can be expressed as follows:

$$y = a + b x + \epsilon \tag{4}$$

where: y—is the dependent variable, X—is the independent variable, a—intercept. b—slope, and ϵ—residual (error).

Another factor of importance is the correlation coefficient, R^2, which measures the degree of association of data. It ranges from + 1 through 0 to − 1. The complete correlation is expressed by the plus and minus unity. The increase in the dependent and independent variables is indicated by the positive value, whereas the negative value indicates the increase in one value with a decrease in the other. It can be calculated as:

$$R^2 = \frac{n(\sum xy) - (\sum x)(\sum y)}{\sqrt{[n(\sum x^2 - (\sum x)^2)]n(\sum y^2 - (\sum y)^2)}} \tag{5}$$

where n is the number of data.

Experimental measurements are taken under similar conditions for the different modes of operation. Therefore, in terms of comparisons, it is assumed that any factors that affect the experimental measurements would equally apply to each mode of operation. As such, any such errors would not affect the results of this study. However, the following broad assumptions are taken:

(i) There is no heat transfer through the surfaces of the experimental test rig since the surfaces are insulated.

(ii) The temperature of the thin layer of water and the plates of the heat exchanger are uniform.

(iii) Mass and heat exchange processes within the test rig are assumed to be steady.

(iv) The wet channels of the plate heat exchanger are thoroughly wetted by the water shower when it is in use.

(v) There is no infiltration or air leakage through joints of the experimental test rig.

(vi) Any unintentional heat transfer or short-circuiting between the primary and secondary air streams are neglected.

4. Results and discussion

The performance of the new air conditioning unit is evaluated by investigating the effect of ambient temperature and humidity on the temperature difference across the heat exchanger, T_{HX}. The obtained results from the experimental analysis are presented and discussed in the following sections.
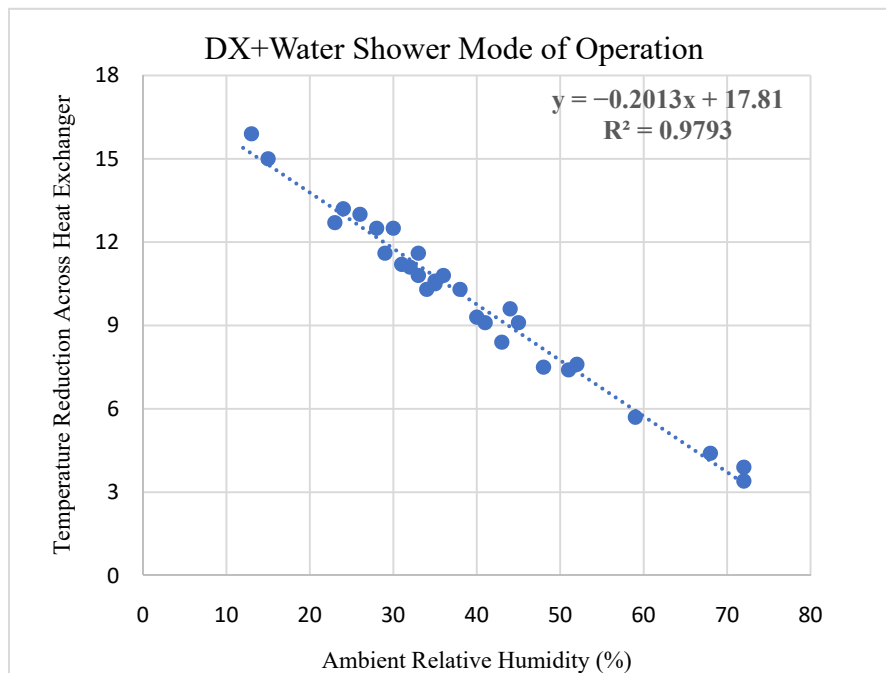
4.1. Variation of T_{HX} with ambient temperature and relative humidity

Figure 2 shows the effect on T_{HX} of increasing ambient dry bulb temperature when the unit operates with the DX and water shower cooling cycles. It was noticed that the relative humidity was in the range of 20–40% in most days of the experiment. In Qatar, the weather condition during summer is characterized by high temperature and relatively low relative humidity except for a few days. The relative humidity is in the range of 20–40%. Therefore, in this analysis, the effect of ambient temperature on T_{HX} is carried out for these relative humidity ranges. As can be seen from the Figure, an increase in ambient dry-bulb temperature improves the temperature reduction of the primary air stream across the heat exchanger. The highest experimentally measured T_{HX} is found to be 15.9 °C at the ambient dry-bulb temperature of 45 °C, while the lowest is 3.4 °C, which occurred at an ambient dry-bulb temperature of 33.5 °C.
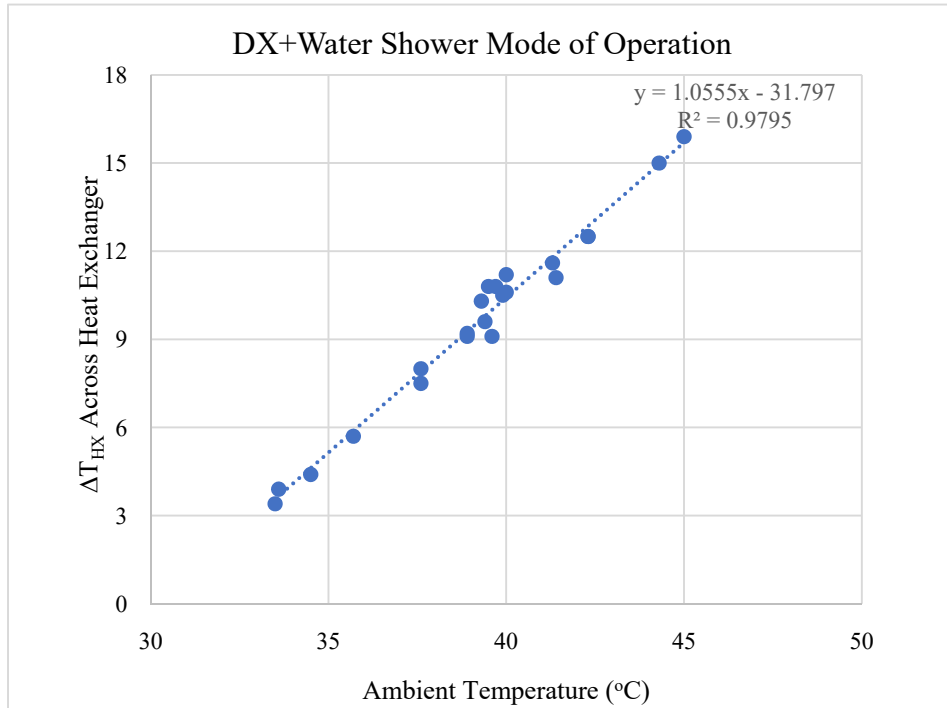
Figure 2. Variation of T_{HX} with the ambient temperature.

Similarly, Figure 3 shows the effect of increasing ambient relative humidity on T_{HX} when the unit operates with the DX and water shower cooling cycles. It can be seen that the majority of the experimental data is in the range of 20–40% relative humidity. The temperature reduction of the primary air stream has a reducing trend as relative humidity increases.

Figure 3. Variation of T_{HX} with ambient relative humidity.

Values of T_{HX} obtained from the linear regression equations shown in Figures 2 and 3 are compared with experimentally measured temperature reductions across the heat exchanger. The linear regression equation of the T_{HX} as a function of ambient temperature is:

$$\Delta T_{HX} = 1.0555\, T_a - 31.797 \tag{6}$$

where T_a is the ambient temperature, and the R^2 value is 09795, which represents smaller differences between the measured data and the fitted values.

The linear regression equation of the T_{HX} as a function of relative humidity is:

$$\Delta T_{HX} = -0.2013\, RH + 17.81 \tag{7}$$

where RH is the relative humidity, and the R^2 value is 09793. The obtained data for T_{HX} using Eqs (6) and (7) is compared to experimentally obtained data. The comparison is made for a small sample of typical ambient conditions to determine which trend best represents the actual temperature reduction across the IEC heat exchanger in the unit. Table 2 shows the results of the comparison.

**Table 2.** Comparison of measured and calculated T_{HX}.

Experimentally Measured			Calculated Parameters			
Ambient Dry-Bulb Temperature (°C)	Ambient Relative Humidity (%)	T_{HX} (a)	T_{HXT} From Temperature Correlation (b)	((b−a)/a) (%)	T_{HXR} From RH Correlation (c)	((c−a)/a) (%)
33.5	72	3.4	3.56	4.77	3.32	−2.46
35.7	59	5.7	5.88	3.23	5.93	4.09
37.6	48	7.5	7.89	5.20	8.15	8.63
42.3	30	12.5	12.85	2.81	11.77	−5.83
45.0	13	15.9	15.70	−1.25	15.19	−4.45

It is found that the deviations between measured values of T_{HX} and those calculated from the linear regression equations (Figures 2 and 3) are less than 10% in all cases. The correlation of T_{HX} with ambient temperature gives a better approximation than does the relationship with ambient relative humidity. Therefore, for the unit, it is better to estimate T_{HX} from the temperature correlation equation.

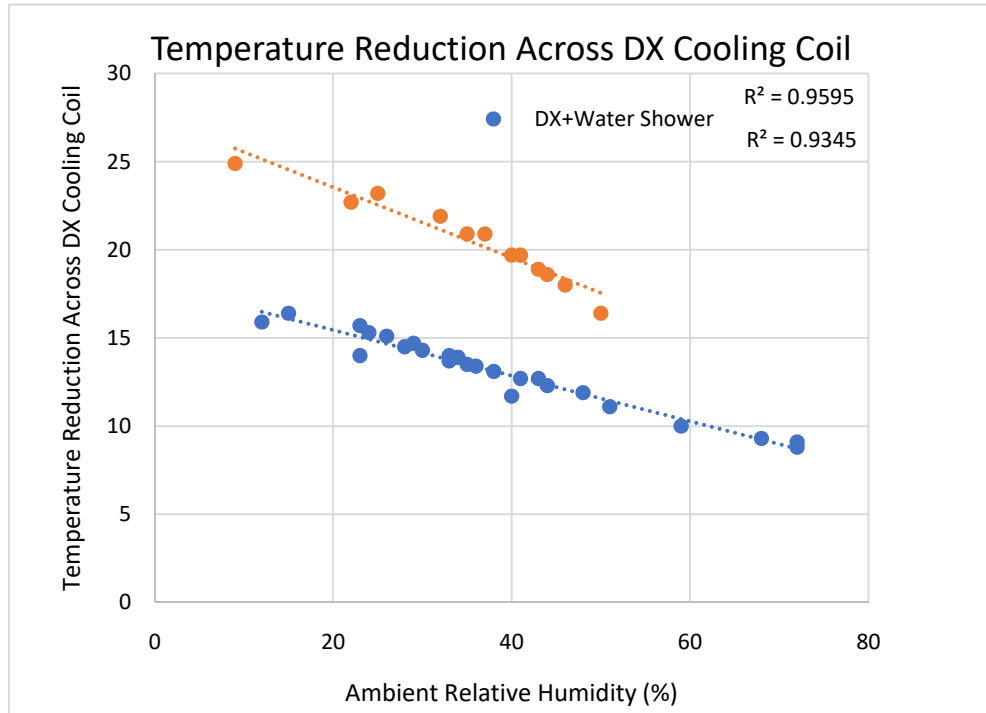## 4.2. Variation of T_{DX} with ambient temperature and relative humidity

Figure 4 shows that the temperature reduction across the DX cooling coil (T_{DX}) increases when the ambient temperature increases for both the DX only and DX with water shower modes of operation. For the variation of T_{DX} with ambient dry-bulb temperature, the results suggest that for the unit, there is a constant difference of about 7.5 °C in the temperature of the primary air stream between the two modes of operation for the given operating conditions. The temperature difference T_{DX} is directly proportional to the sensible cooling load across the DX cooling coil. Over the experimental operating conditions, this suggests that when the ambient temperature is 37 °C, the DX with water shower mode would require about 67% less temperature reduction (i.e., sensible cooling) across the DX cooling coil than does the DX only mode of operation. At an ambient temperature

of 45 °C, the saving in temperature reduction (sensible cooling) amounts to 50.6%, compared to that required by the DX only mode to achieve the same supply air setpoint.
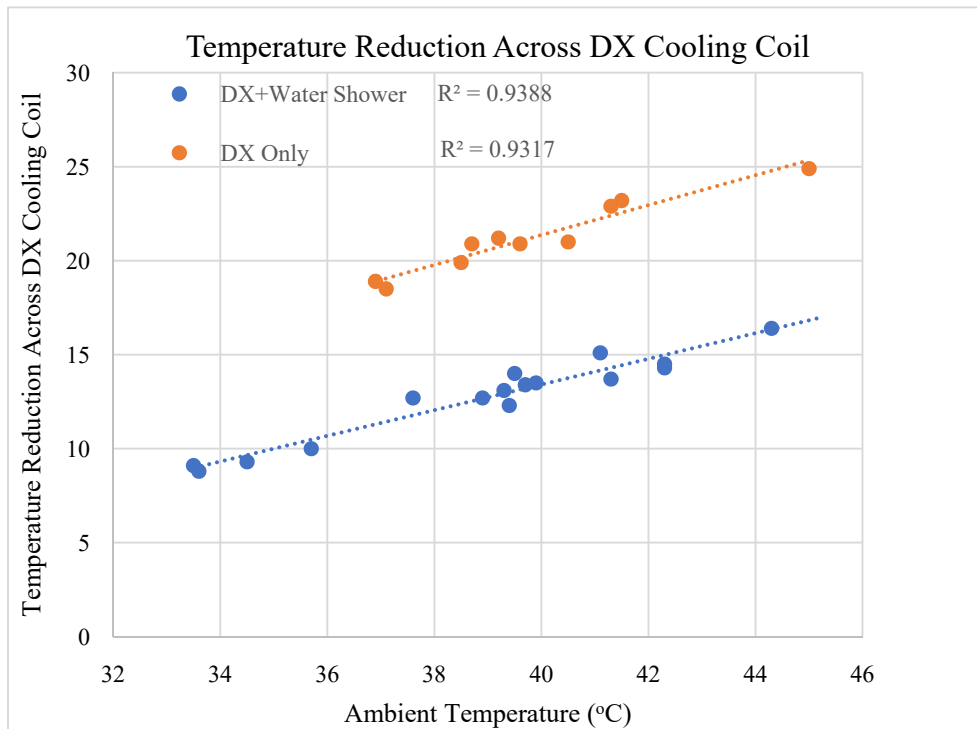
Figure 4. Variation of T_{DX} with the ambient temperature.

However, when the variation of T_{DX} is considered against the ambient relative humidity (Figure 5), the difference in a temperature reduction of the primary air stream across the DX cooling coil, for the two modes of operation, decreases with increasing relative humidity. It is determined from Figure 5 that when the ambient relative humidity is ten % RH, the DX with water shower requires 52.5% temperature reduction (sensible cooling) across the DX cooling coil, which reduces slightly to 51.8% when the ambient relative humidity is 50% RH, compared to the amount of sensible cooling required by the DX only mode of operation.

Figure 5. Variation of T_{DX} with ambient relative humidity.

Figure 6 shows the variation of the unit COP with ambient dry-bulb temperature. It is found that the use of the water shower improves the COP of the unit. The difference between the COPs of the two modes of operation remains constant with increasing ambient dry-bulb temperature. The highest COP of the DX with water shower mode is found to be 3.45, while that of the DX only mode is found to be 2.07. As ambient dry bulb temperature increases, more evaporation of water is expected to occur, which would increase the evaporative cooling performance of the unit and reduces the cooling load on the DX cooling coil.
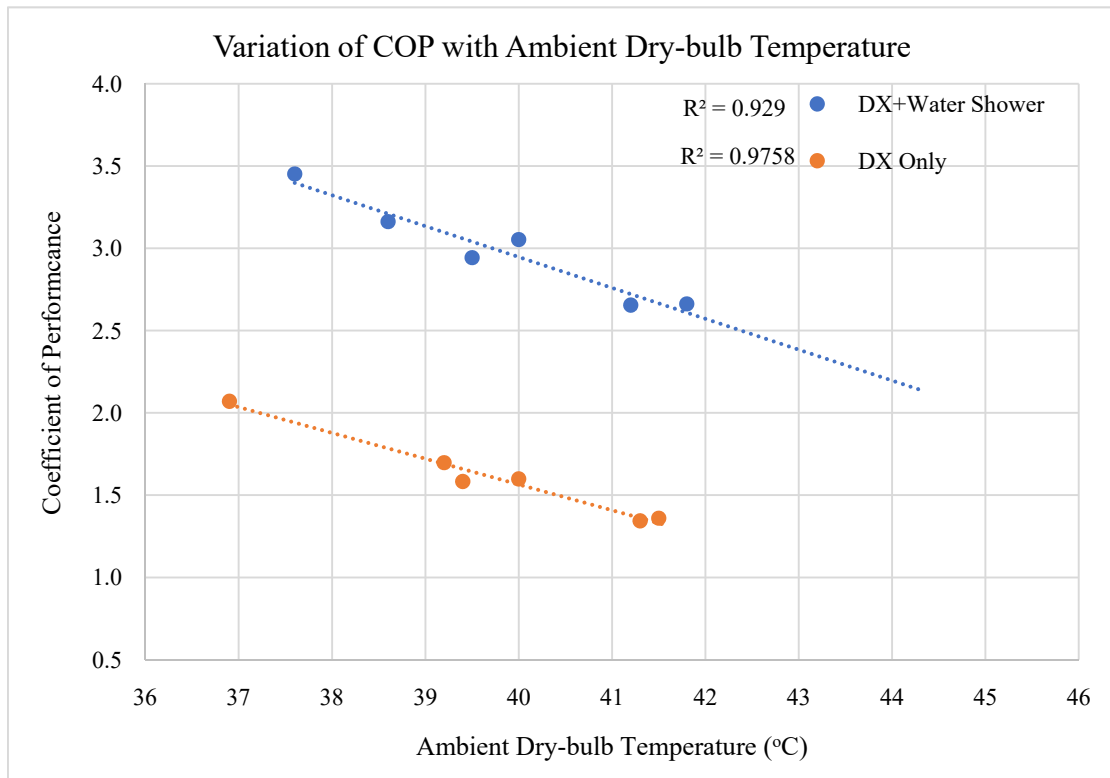
Figure 6. Variation of COP with ambient dry bulb temperature.

The cooling performance of the unit was also considered by calculating the wet-bulb thermal effectiveness of the heat exchanger. As expected, the cooling capacity of the unit increases with increasing wet-bulb thermal effectiveness of the IEC heat exchanger. With an increase of wet-bulb thermal effectiveness from 0.4 to 0.8, it was found that the COP increases by approximately 14.5%, while the cooling capacity increases by 8.8%. For both the COP and cooling capacity to increase over a given range of wet-bulb thermal effectiveness, it means the power consumption associated with increasing wet-bulb thermal effectiveness of the unit from 0.4 to 0.8, must therefore decrease.

Figure 7 illustrates the decreasing trend of variation of wet-bulb thermal effectiveness with dry-bulb temperature. The trends are represented by polynomial regression curves for which excellent correlation coefficients were obtained. For ambient relative humidity greater than 30% RH, the curves merge at a dry-bulb temperature of 31.8 °C. The trends also show that the wet-bulb thermal effectiveness of the unit improves with increasing ambient relative humidity. Figure 7 also suggests that the unit has its lowest limiting wet-bulb thermal effectiveness when the ambient dry-bulb temperature reaches 31.8 °C in ambient conditions with relative humidity above 30% RH.
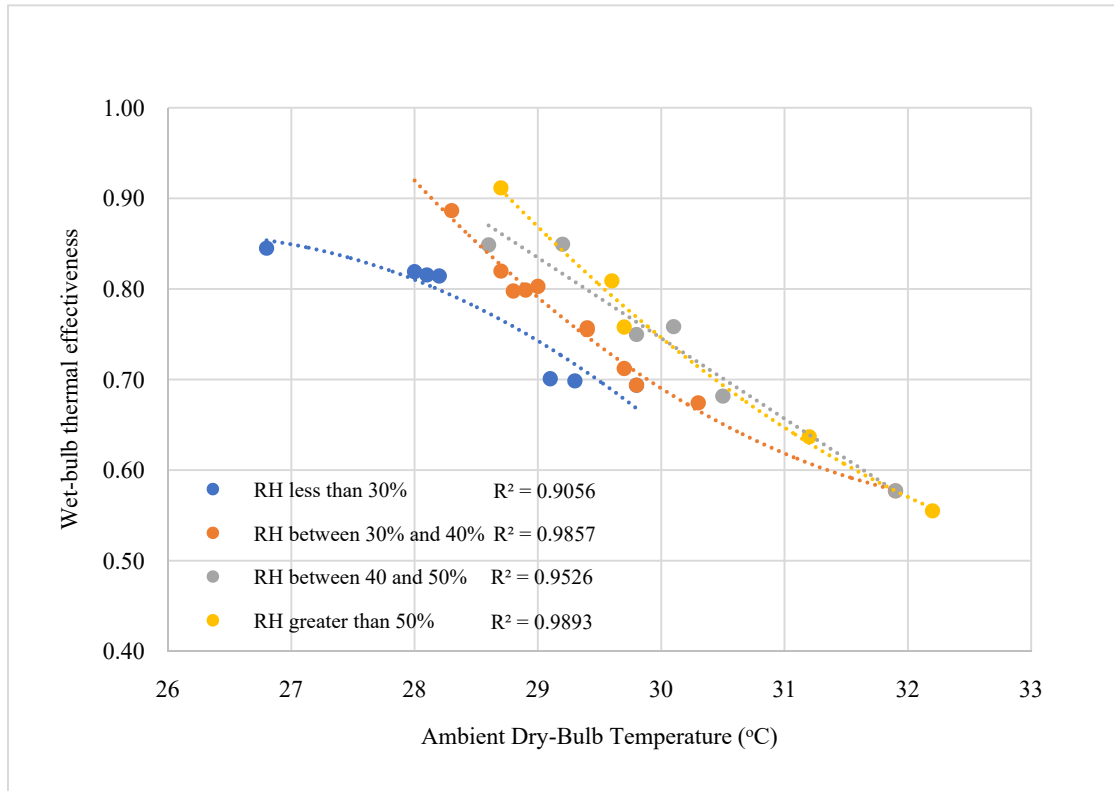
Figure 7. Variation of wet-bulb thermal effectiveness with ambient dry-bulb temperature.

An illustration of the variation of the wet-bulb thermal effectiveness of the unit with ambient wet-bulb temperature is shown in Figure 8. In general, the unit achieves given effectiveness at higher temperatures in more humid conditions than it does in lower relative humidity conditions. Also, for the given operating conditions, at a given wet-bulb temperature, the unit achieves higher wet-bulb thermal effectiveness in less humid conditions.
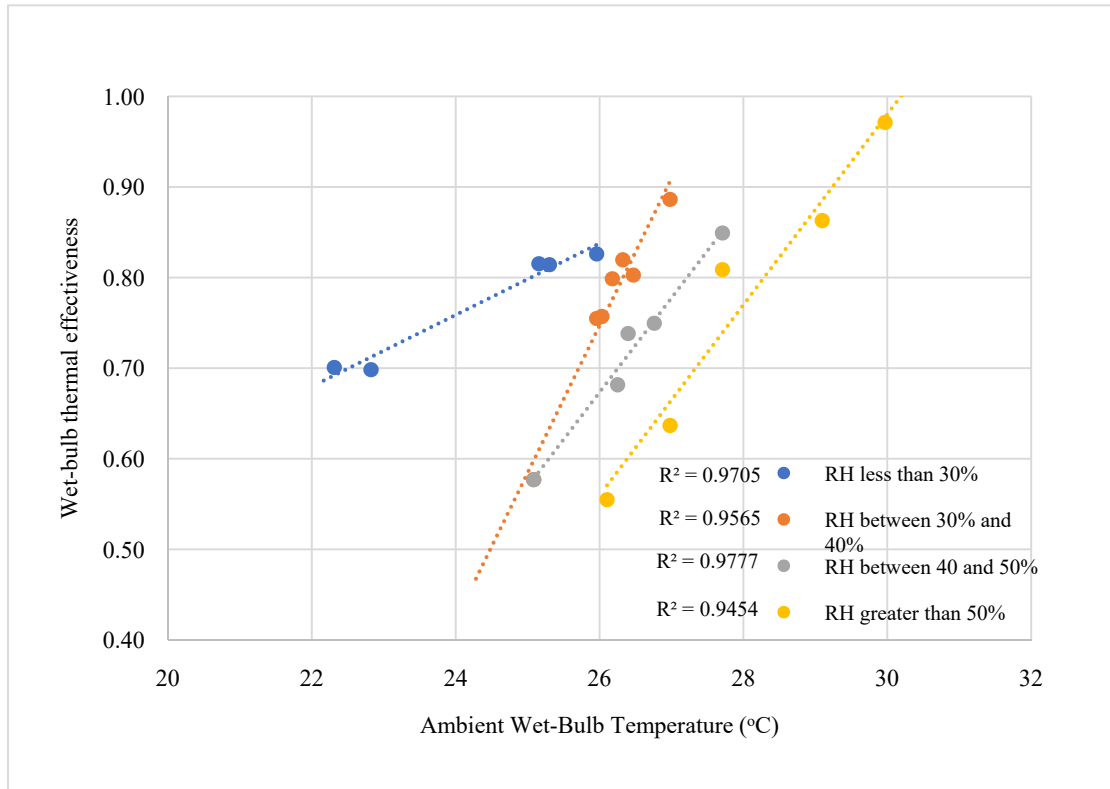
Figure 8. Variation of wet-bulb thermal effectiveness with wet bulb temperature.

The variation of T_{HX} with wet-bulb thermal effectiveness is such that T_{HX} increases with increasing wet-bulb thermal effectiveness. As T_{HX} increases, the load on the DX cooling coil reduces, and this leads to the unit requiring less energy to drive the compressors than it does in the DX only mode of operation.

4.3. Comparison of total cooling loads between two modes of operation

In the air handling cooling unit, the total cooling load is shared between the indirect evaporative cooling heat exchanger and the DX cooling coil. However, in the practice part, the cooling capacity of the machine is lost in of-setting losses, such as the heat gain across the supply air fan. Table 3 shows the total cooling loads calculated using equation 2 for the two modes of operation when working in various ambient conditions. In Table 3, a small sample of selected representative ambient conditions is used as the basis of comparison. The actual temperatures and relative humidity measured during the experiments, from which the representative ambient conditions are approximated, are included in Table 3.

Table 3. Total cooling loads at various ambient conditions.

Representative Ambient Conditions	Mode of Operation	Measured Temperature (°C)	Measured RH (%)	Total Cooling Load (kW)	Cooling Load on HX (kW)	Cooling Load on DX Coil (kW)	Saving in Cooling Load (%)
41 °C/25% RH	DX	41.5	25	91.26	10.92	80.34	35.28
	DX+WS	41.2	25	113.25	53.86	59.39	
39.4 °C/35% RH	DX	39.1	35	94.66	3.67	90.99	26.80
	DX+WS	39.6	35	116.21	44.45	71.76	
38.5 °C/50% RH	DX	37.8	52	82.37	1.20	81.17	19.35
	DX+WS	39.1	51	96.73	28.72	68.01	

For the given ambient conditions, the cooling performance, in terms of the total cooling load, of the unit increases when operating with the IEC cycle. For instance, in relatively dry ambient conditions (41 °C/25% RH), the unit provides 113.25 kW with the IEC cycle compared to 91.26 kW when the DX cooling cycle operates alone. The contribution of the IEC cycle to the total cooling ability of the unit diminishes with increasing ambient relative humidity. This behavior is expected, as can be seen from Figure 3, which shows a reduction in T_{HX} as ambient relative humidity increases. It is found that when using the DX with water shower mode in relatively dry ambient conditions (41 °C/25% RH), the DX cooling cycle provides 52% of the total cooling requirement. The contribution of the DX cooling cycle increases as ambient conditions become more humid, i.e., reaching 70% when ambient conditions are 38.5 °C and 50% RH. The amount of the total cooling load saved with the use of the water shower at various ambient conditions is given in Table 3. For the representative ambient conditions selected for comparison, the saving in total cooling load is 35.28% in dry conditions (41 °C/25% RH), which decreases to 19.35% in ambient conditions of 38.5 °C and 50% RH.

4.4. Comparison of power consumption between two modes of operation

The experimentally measured power consumption of the unit, when operating with only the DX cycle, and that required for the combined DX and water shower at several representative ambient conditions are presented in Table 4. The representative ambient conditions are approximated from actual experimentally measured parameters (also shown in Table 4). For the range of parameters considered, the highest power consumption of the unit, when operating with the DX cooling cycle only, is 49.96 kWh, which occurred in ambient conditions of 39.7 °C and 34.5% RH. The corresponding power consumption when working with the combined DX and water shower mode is 33.34 kWh.

Table 4. Power and water consumptions at various ambient conditions.

Representative Ambient Conditions	Mode of Operation	Measured Temperature (°C)	Measured RH (%)	Power Consumption (kWh)	Condensate Generated (kg/h)
43 °C/15% RH	DX	41.30	15.00	45.74	0.00
	DX + WS	44.30	15.00	31.87	-
42 °C/25% RH	DX	41.60	25.00	43.33	0.00
	DX + WS	41.80	26.00	32.26	0.00
39.7 °C/33% RH	DX	39.70	34.50	49.96	33.08
	DX + WS	39.75	32.00	33.34	42.50
39 °C/28% RH	DX	39.90	22.00	45.83	32.00
	DX + WS	38.60	34.00	34.84	42.00
39 °C/37% RH	DX	39.20	36.00	45.68	30.00
	DX + WS	39.30	38.00	33.50	-
37 °C/45% RH	DX	36.90	43.00	44.80	52.63
	DX + WS	37.60	48.00	32.88	56.00

A comparison of the power consumption can be seen in Figure 9. It is found that the unit consumes more power when operating with the DX cycle than when it engages with the DX and water washer in combination. Using the water shower provides a saving in power consumption, which reduces with increasing ambient relative humidity for a given temperature. The most significant saving in power consumption, based on the representative ambient conditions, is found to be 49.85%, at an ambient temperature of 39.7 °C, and relative humidity of 33%. The saving in power consumption reduces to 43% in dry ambient conditions of 43 °C and 15% relative humidity. At 37 °C and 45% RH, the power saving is 36.3%.
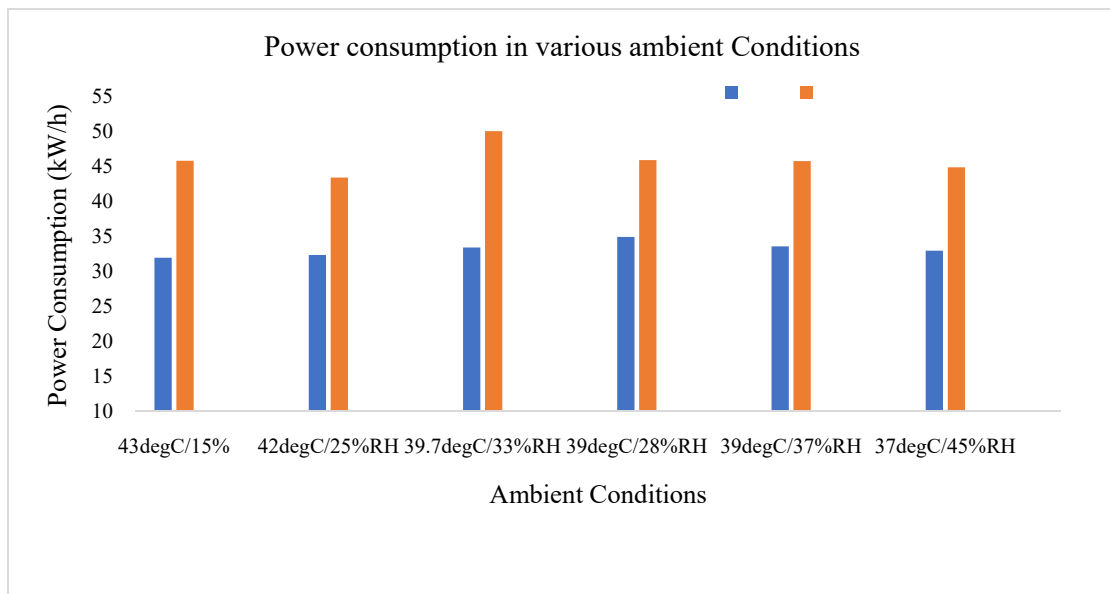

Figure 9. Comparison of power consumptions at various ambient conditions.

4.5. Condensate generation by DX cooling coil

Another attractive feature of the unit machine is that, depending on ambient conditions, it can generate enough quantities of condensate that can be reused for indirect evaporative cooling purposes, thus eliminating or significantly reducing the amount of potable water required. This potential to save water adds to enhance the sustainability credentials of the unit technology. The quantity of condensate generated by the unit when operating, in DX only and DX with water shower modes of operation, at typical ambient conditions is presented in Table 4.

Studies are scarce, in the literature, done to quantify the self-sufficiency of IEC systems concerning water consumption, and by considering condensate generation capabilities. Figure 10 shows an assessment of the condensate generation rates of the unit when it operates in the DX only and the DX with water shower modes.
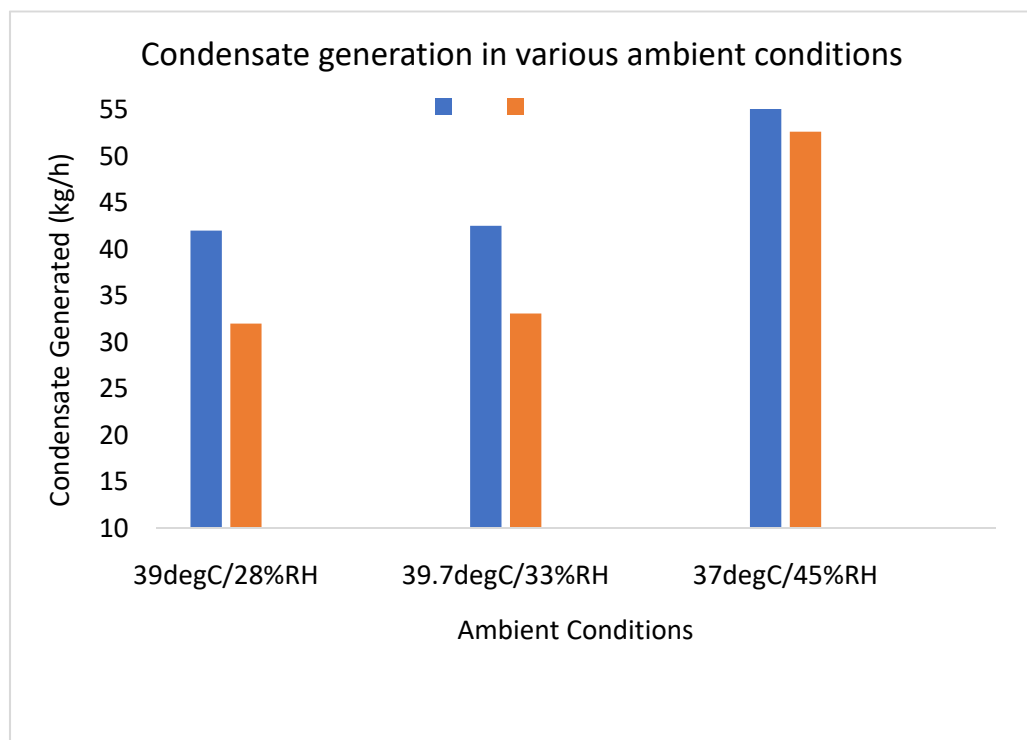
Figure 10. Comparison of condensate generation rates.

It is found that across the range of selected representative ambient conditions, the DX with water shower mode of operation generally generates more condensate than the DX only mode when ambient conditions permit. In the experimental operating conditions, the highest condensate generation rate of the DX with water shower mode is found to be 56 kg/h, while that of the DX, the only mode is 52.63 kg/h, both occurring in ambient conditions of 37 °C and 45% RH. In drier ambient conditions, the unit generates 31.3% more condensate with the DX with water shower mode than it does with the DX, the only mode of operation. For similar ambient dry-bulb temperature, the unit generates more condensate when the ambient relative humidity is higher.

An earlier study by researchers at GORD suggested that the average amount of water needed for indirect evaporative cooling in a diverse range of ambient conditions by a similar fresh air handling

unit, of half the airflow capacity of the unit is around 20–22 kg.h. It is reasonable, therefore, to state that the unit can successfully off-set its potable water consumption when ambient conditions permit.

As the wet-bulb thermal effectiveness of the heat exchanger increases, the rate of condensate generation would decrease for given operating conditions. The decrease in the rate of condensate generation is because, as the wet-bulb thermal effectiveness of the heat exchanger increases, the IEC heat exchanger provides more cooling of the primary airstream. Hence, the cooling load imposed on the DX cooling coil is reduced, leading to the reduced potential of condensate generation. There is, therefore, a conflict between the factors that influence the cooling performance and water sustainability aspects of the unit. For instance, when wet-bulb thermal effectiveness increases, the temperature reduction across the heat exchanger increases, as does the cooling load/COP, while the ability of the unit to generate condensate, which could be used for the IEC cycle, diminishes. There must, therefore, be a compromise point at which the unit provides net benefit from both the energy-saving and water-saving perspectives. However, determination of such an optimized point of operation is outside the scope of the present study.

4.6. System energy performance assessment

Researchers used several techniques to evaluate the performance of new refrigeration cycles and equipment, including payback period, net present value, return on investment, COP, energy efficiency ratio (EER), and seasonal energy efficiency ratio (SEER) [35–37]. In the present work, the energy savings assessment of the new technology will be carried out using COP, EER, and SEER. The EER is related to the COP as follows:

$$EER = 3.41 * COP \tag{8}$$

The SEER is usually used to estimate the relative amount of energy needed to provide a specific cooling output, and it is expressed in BTU/Wh. It represents the expected overall performance for a typical year's weather in a given location, and it is evaluated at the same indoor temperature, but over a range of outside temperatures of (18–40) °C the relationship between EER and SEER is as follows:

$$SEER = \left(1.12 - \sqrt{(1.2544 - 0.08 * EER)}\right)/.04 \tag{9}$$

The values of COP, EER, and SEER For the tow modes of operation at three climate conditions are presented in Table 5.

Table 5. Performance characteristics of the operational modes.

Ambient conditions	DX			Dx + WS		
	COP	EER	SEER	COP	EER	SEER
41 °C/25% RH	2.11	7.18	7.39	3.51	12.64	15.67
39 °C/30% RH	1.89	6.46	6.53	3.48	12.55	15.49
37 °C/48% RH	1.83	6.27	6.31	2.94	10.6	12.05

It is clear that the SEER value of the new unit with DX and water shower mode has been doubled for all ambient conditions considered. The power consumption of the air conditioning unit is estimated as (1-SEER$_{DX}$/SEER$_{DXWS}$). For the values under consideration, the savings are in the range

of 47.6–52.8%. The actual annual saving for the unit is estimated at the cost of $0.09/kWh and is found to be $6,415.

5. Conclusions

Naturally, there is a conflict between parameters promoting energy-saving and condensate generation (to offset or replace potable water use), hence a compromise between opposing operating parameters should be established. This study was set out to experimentally investigate the cooling performance of a patented air conditioning unit with new technology and considered various parameters affecting cooling performance as well as condensate water generation by the cooling cycles. Temperature and relative humidity were measured and recorded at the main points of the air conditioning unit and logged with a wireless data acquisition system. Linear regression analysis was implemented to the obtained experimental data, and the correlation coefficient was determined. The wet-bulb thermal effectiveness, cooling capacity, and system COP were calculated to evaluate the system performance. The results showed that the new unit had a peak wet-bulb thermal effectiveness and a COP of 1.3 and 3.4, respectively.

In addition, it was found that:

- The EC cycle could reduce the temperature of the primary airstream by up to16 ℃ in ambient temperatures higher than 40 ℃.
- For the experimental operating conditions, when the unit utilized the IEC cycle, the sensible cooling load on the DX cooling coil was reduced by 67% while the total cooling load was reduced by 38.5%, depending on ambient conditions.
- Also, it was deduced that the air conditioning unit could provide savings up to 36% in power consumption by using the IEC cycle, in comparison to cooling using only the DX vapor compression cycle.
- The new technology generated enough condensate to meet the water requirements of the IEC cycle. For instance, in ambient conditions of 37 ℃ and 45% RH, the unit produced 56 kg.hr^{-1} of condensate when operating with the DX with a water shower mode of operation.

Acknowledgments

Conflict of interest

The authors declare no conflict of interests.

References

1. Pinar M, Riffat S (2016) A state-of-the-art review of evaporative cooling systems for building applications. *Renewable Sustainable Energy Rev* 54: 1240–1249.
2. Baniassadi A, Hensinger J, Sailor D (2018) Building energy savings potential of hybrid roofing system involving high albedo, moisture-retaining foam materials. *Energy Build* 169: 283–294.

3. Tashtoush B, Bani Younes M (2019) Comparative thermodynamic study of refrigerants to select the best Environment-Friendly refrigerant for use in a solar ejector cooling system. *Arab J Sci Eng* 44: 1165–1184.

4. Al Shahrani J, Boait P (2019) Reducing high energy demand associated with air conditioning needs in Saudi Arabia. *Energies* 13: 87.

5. Elakhdar M, Tashtoush B, Nehdi E, et al. (2018) Thermodynamic analysis of a novel Ejector Enhanced Vapor Compression Refrigeration (EEVCR) cycle. *Energy* 163: 1217–1230.

6. Megdouli K, Tashtoush B, Nahdi E, et al. (2016) Thermodynamic analysis of a novel ejector-cascade refrigeration cycles for freezing process applications and air-conditioning. *Int J Refrig* 70: 108–118.

7. Elakhdar M, Landoulsi H, Tashtoush B, et al. (2017) A combined thermal system of ejector refrigeration and Organic Rankine cycles for power generation using a solar parabolic trough. *Energy Convers Manage* 199: 111947.

8. Tashtoush BM, Al-Nimr MA, Khasawneh MA (2017) Investigation of the use of nano-refrigerants to enhance the performance of an ejector refrigeration system. *Appl Energy* 206: 1446–1463.

9. Porumb B, Unguresan P, Tutunaru L, et al. (2016) A review of indirect evaporative cooling conditions and performances. *Energy Procedia* 85: 452–460.

10. Al Horr Y, Tashtoush B, Chilengwe N, et al. (2019) Performance assessment of a hybrid vapor compression and evaporative cooling fresh-air-handling unit operating in hot climates. *Processes* 7: 872.

11. Duan Z, Zhan C, Zhang X, et al. (2012) Indirect evaporative cooling: Past present and future potentials. *Renewable Sustainable Energy Rev* 16: 6823–6850.

12. De Antonellis S, Joppolo C, Liberati P (2019) Performance measurements of a cross-flow indirect evaporative cooler: Effect of water nozzles and airflow arrangement. *Energy Build* 184: 114–121.

13. Cui X, Chua K, Yang W (2014) Use of indirect evaporative cooling as pre-cooling unit in humid tropical climate: an energy saving technique. *Energy Procedia* 61: 176–179.

14. Pandelidis D, Anisimov S, Drag P (2017) Performance comparison between selected evaporative air coolers. *Energies* 10: 577.

15. Tashtoush B, Abu-Irshaid E (2001) Heat and fluid flow from a wavy surface subjected to a variable heat flux. *Acta Mech* 152: 1–8.

16. Rogdakis E, Tertipis D (2015) Maisotsenko cycle: technology overview and energy-saving potential in cooling systems. *Energy Emiss Control Technol* 3: 15–22.

17. Moshari S, Heidarinejad G (2015) Numerical study of regenerative evaporative coolers for sub-wet bulb cooling with cross- and counter-flow configuration. *Appl Therm Eng* 89: 669–683.

18. Chen Y, Yang H, Luo Y (2017) Parameter sensitivity analysis and configuration optimisation of indirect evaporative cooler (IEC) considering condensation. *Appl Energy* 194: 440–453.

19. Gomez E, Gonzalez A, Martinez F (2012) Experimental characterisation of an indirect evaporative cooling prototype in two operating modes. *Appl Energy* 97: 340–346.

20. Tashtoush B, Tahat M, Al-Hayajneh A, et al. (2001) Thermodynamic behaviour of an AC system employing combined evaporative-water and air coolers. *Appl Energy* 70: 305–319.

21. Chen Y, Yang H, Luo Y (2016) Experimental study of plate type air cooler performances under four operating modes. *Build Environ* 104: 296–310.

22. El Dessouky H, Ettouney H, Al-Zeefari A (2004) Performance analysis of two-stage evaporative coolers. *Chem Eng J* 102: 255–266.

23. Rajski K, Danielewicz J, Brychcy E (2020) Performance evaluation of a Gravity-Assisted heat Pipe-Based indirect evaporative cooler. *Energies* 13: 200.

24. Saman W, Alizadeh S (2002) An experimental study of a cross-flow type plate heat exchanger for dehumidification/cooling. *Sol Energy* 73: 59–71.

25. Zhan C, Duan Z, Zhao X, et al. (2011) Comparative study of the performance of the M-Cycle counter-flow and cross-flow heat exchanger for indirect evaporative cooling—paving the path toward sustainable cooling of buildings. *Energy* 36: 6790–6805.

26. Al Zubaydi A, Hong G (2019) Experimental study of a novel water spraying configuration in indirect evaporative cooling. *Appl Therm Eng* 151: 283–293.

27. Zhao X, Liu S, Riffat S (2008) Comparative study of heat and mass exchanging materials for indirect evaporative cooling systems. *Build Environ* 43: 1902–1911.

28. Al Juwayhel F, El-Dessouky H, Ettouney H, et al. (2004) Experimental evaluation of one, two and three-stage evaporative cooling systems. *Heat Trans Eng* 25: 72–86.

29. Maheshwari G, Al Ragom F, Suri R (2001) Energy-saving potential of an indirect evaporative cooler. *Appl Energy* 69: 69–76.

30. Delfani S, Esmaeelian J, Pasdarshahri H, et al. (2010) Energy-saving potential of an indirect evaporative cooler as a pre-cooling unit for mechanical cooling systems in Iran. *Energy Build* 42: 2169–2176.

31. Chauhan S, Rajput S (2015) Thermodynamic analysis of the evaporative vapour compression based combined air conditioning system for hot and dry climatic conditions. *J Build Eng* 4: 200–208.

32. Kim M, Jeong J (2013) Cooling performance of a 100% outdoor air system integrated with indirect and direct evaporative coolers. *Energy* 52: 245–257.

33. Porumb B, Balan M, Porumb R (2016) Potential of indirect evaporative cooling to reduce energy consumption in fresh air conditioning applications. *Energy Procedia* 85: 433–441.

34. Tashtoush B, Al-Oqool A (2019) Factorial analysis and experimental study of water-based cooling system effect on the performance of photovoltaic module. *Int J Environ Sci Technol* 16: 3645–3656.

35. Megdouli K, Tashtoush B, Ezzaalouni Y, et al. (2017) Performance analysis of a new ejector expansion refrigeration cycle (NEERC) for power and cold: Exergy and energy points of view. *Appl Therm Eng* 122: 39–48.

36. Karali N, Shah N, Park W, et al. (2020) Improving the energy efficiency of room air conditioners in China: Costs and benefits. *Appl Energy* 258: 114023.

37. Tashtoush B, Nayfeh Y (2020) Energy and economic analysis of a variable-geometry ejector in solar cooling systems for residential buildings. *J Energy Storage* 27: 101061.